Phyton-
International Journal of
Experimental Botany

Tech Science Press

http://doi.org/10.32604/phyton.2026.079359

ARTICLE

Physiological Mechanisms and Application Potential of Nano-Zinc Oxide in Alleviating Saline-Alkali Stress in Sorghum

Haoran Li, Qi Sun, Haoran Sun, Ziyan Wu, Wenjin Wang and Fang Liu*

School of Resources and Environmental Engineering, Inner Mongolia University of Technology, Hohhot, China
*Corresponding Author: Fang Liu. Email: lf781031@163.com

Received: 20 January 2026; Accepted: 25 March 2026; Published: 28 April 2026

ABSTRACT: Soil salinization is an increasingly severe global issue, posing a significant threat to crop growth and food security. Although sorghum exhibits moderate tolerance to saline-alkali stress, it remains highly sensitive to such conditions during the seedling stage. This study investigates the mechanisms by which zinc oxide nanoparticles (ZnO NPs) alleviate saline-alkali stress in sorghum seedlings and determines their optimal application concentration, thereby providing a scientific basis for agricultural production in saline-alkali soils. Hydroponic experiments were conducted to simulate varying degrees of saline-alkali stress. Sorghum seedlings were treated with different concentrations of ZnO NPs (0, 50, 100, 200 mg·L^{-1}). The efficacy of ZnO NPs was comprehensively evaluated by measuring biomass, chlorophyll content, antioxidant enzyme activities, non-enzymatic antioxidant levels, sodium and potassium ion distribution, and lipid peroxidation. These physiological assessments were further supported by correlation analysis, principal component analysis (PCA), and response surface methodology (RSM). The results indicate that ZnO NPs maintain intracellular redox homeostasis by inhibiting the degradation of photosynthetic pigments, enhancing the synergistic interactions between enzymatic and non-enzymatic antioxidants, and preserving ionic equilibrium. These mechanisms effectively suppress malondialdehyde accumulation, protect membrane integrity, and improve seedling resilience to stress. Furthermore, PCA and RSM revealed that the optimal ZnO NPs concentration is approximately 100 mg·L^{-1}. Excessive concentrations, however, exert toxic effects and inhibited seedling growth. Overall, this study highlights the potential of applying ZnO NPs as nano-fertilizers to improve crop resilience in saline-alkali soils.

KEYWORDS: ZnO NPs; abiotic stress; sorghum; plant physiology; response surface analysis

1 Introduction

Soil salinization poses an increasingly severe threats to global arable land. According to the Food and Agriculture Organization of the United Nations (FAO), the global area of salt-affected soils has surpassed 833 million hectares, accounting for approximately 8.7% of the world's total land area [1]. Furthermore, factors such as drought and unsustainable irrigation practices are driving the rapid expansion of saline-alkali soils [2]. Projections indicate that without effective countermeasures, approximately 50% of global arable land may lose productivity due to secondary salinization by 2050, posing a significant threat to global food security [3]. In agricultural contexts, it is crucial to distinguish between salt stress and alkali stress. Although these conditions frequently co-occur, alkali stress (primarily driven by $NaHCO_3$ and Na_2CO_3) is significantly more detrimental to plants growth than neutral salt stress (induced by NaCl and Na_2SO_4). Unlike salt stress, which primarily inflicts osmotic stress and ion toxicity, alkali stress introduces the compounding, lethal factor of high soil pH (>8.5) [4]. Elevated pH environments compromise the integrity of root epidermal cells

and trigger the precipitation of essential trace metals (such as Fe^{2+}, Zn^{2+}, Mn^{2+}) as insoluble hydroxides in the rhizosphere. This severely reduces their bioavailability, thereby inducing acute nutrient deficiency [5]. Consequently, numerous studies have confirmed that at equivalent ion concentration, alkaline stress exerts a substantially stronger inhibitory effects on crop root activity, photosynthetic efficiency, and overall biomass accumulation than salt stress [6,7].

Nanotechnology has emerged as a highly promising strategy for enhancing crop resilience to abiotic stresses [8–10]. By function as nano-fertilizers or nano-pesticides, nanomaterials can significantly improve nutrient use efficiency while mitigating the negative environmental impacts associated with conventional agricultural inputs [11–13]. Among these, zinc oxide nanoparticles (ZnO NPs) have garnered considerable attention due to their dual benefits. First, zinc (Zn) is an essential plant micronutrient that plays a critical role in enzymes activation, hormone synthesis, membrane stabilization, and the maintenance of redox homeostasis [14]. Second, compared to conventional fertilizers, ZnO NPs possess superior physiochemical properties, including a higher specific surface area and more controlled nutrient release dynamics [15]. Consequently, under various abiotic stresses, ZnO NPs have been shown to effectively interact with plant tissues to modulate ion transport, osmolyte accumulation, reactive oxygen species (ROS) scavenging systems, and the expression of stress-responsive genes, thereby bolstering overall plant stress tolerance [16–18]. Extensive research on diverse crops has demonstrated that the exogenous application of ZnO NPs can significantly mitigate the adverse effects of salt stress. In wheat (*Triticum aestivum*), for instance, the foliar application of ZnO NPs increases chlorophyll content, enhances gas exchange parameters, and improves K^+ uptake capacity. It also boosts antioxidant enzyme activity, which collectively promotes vegetative growth and improves grain yield under saline conditions [19]. Analogous protective effects have been documented in other crops, such as tomato (*Solanum lycopersicum*), pea (*Pisum sativum*), and rice (*Oryza sativa*). In these species, ZnO NPs alleviate salt-induced damage by enhancing photosynthetic performance, fortifying antioxidant defense mechanisms, reducing lipid peroxidation, and restoring both ion balance and osmotic regulation [15,20–23].

Sorghum (*Sorghum bicolor*) ranks as the fifth most important cereal crop globally and plays a pivotal role in ensuring food security, largely due to its exceptional intrinsic stress tolerance [24,25]. Although sorghum is generally classified as moderately salt tolerance, this resilience fluctuates significantly across its developmental stages. Specifically, the seed germination and seedling establishment phases are highly susceptible to saline-alkali environments [26,27]. During this critical developmental window, saline-alkali stress severely reduces seedling emergence rates and inhibits root development. Ultimately, this leads to suboptimal plant density at maturity, resulting in substantial yield penalties [28,29].

Although the growing body of research on nanomaterials for alleviating plant salt stress has provided a solid theoretical foundation for their agricultural application, this field requires further exploration to address complex ecological environments. First, the majority of nanoparticle-salinity studies have primarily focused on the simple osmotic and ionic stresses induced by neutral salts [30,31]. However, in salinized agricultural regions, plants frequently encounter combined saline-alkali stress. Studies by Wang et al. indicate that, compared to single salt stress, the high pH and the presence of carbonates or bicarbonates associated with combined stress induce more severe ion toxicity, root metabolic dysfunction, and reduced nutrient availability [32]. To date, research investigating the mechanisms by which ZnO NPs alleviate combined saline-alkali stress remains relatively limited. Secondly, existing studies exploring the use of nanomaterials to enhance stress resistance in sorghum have largely concentrated on the mid-to-late growth stages and final yield evaluations under high-salinity conditions. Nevertheless, physiological and transcriptomic analyses by Wu et al. have identified the sorghum seedling stage as a physiologically vulnerable window

that is highly sensitive to saline-alkali environments. Morphogenesis and stress resistance during this stage are crucial not only for early plant survival, but also serve as a critical foundation influencing subsequent population structure and yield potential [7,33].

Therefore, in contrast to traditional single-salinity models, this study utilizes realistic combined saline-alkali stress conditions as the research context. Focusing on the critical developmental stage of sorghum seedlings, we investigated the effects of various ZnO NPs treatments on their growth, photosynthetic characteristics, and key stress-related physiological and biochemical indices. Given the physicochemical properties of nanomaterials and their potential roles in plant stress resilience, we hypothesized that the exogenous application of ZnO NPs could alleviate the growth inhibition induced by saline-alkali stress in sorghum seedlings. We further posited that this mitigation is achieved by regulating ion homeostasis, enhancing photosynthetic performance, and remodeling physiological and biochemical responses, and that this effect is highly concentration-dependent. To test this hypothesis, we conducted a comprehensive analysis of multiple parameters, including morphological traits, physiological responses, and ion homeostasis. Specifically, this study aims to: (1) elucidate the effects and underlying mechanisms of ZnO NPs treatments on the growth and physiology of sorghum seedlings; (2) determine the optimal ZnO NPs concentration for mitigating saline-alkali stress damage, thereby providing a theoretical basis for the safe and efficient application of ZnO NPs in sorghum cultivation across salinized soils.

2 Material and Methods

2.1 Experimental Design

The hydroponic experiment was conducted at room temperature from April to May 2025. Sorghum seedlings were grown under natural light conditions with an intensity of approximately 800–1000 μmol·m^{-2}·s^{-1}. Environmental conditions were maintained at day/night temperatures of 26/22°C, a 10/14 h light/dark cycle, and a relative humidity of 60%–70%. Seeds of sorghum variety “Kangsi Gaoliang” were procured from Mengya Seed Sales Co., Ltd. (Hejian City, Hebei Province). Plump seeds were selected, surface-sterilized with a 5% NaClO solution for 20 min, and thoroughly rinsed with distilled water.

The ZnO NPs used in this study were synthesized using sea buckthorn leaf extract. The synthesized nanoparticles exhibited an average particle size of 200 nm and a zeta potential of −44.07 mV, demonstrating good stability. Informed by preliminary experiments and previous studies, ZnO NPs suspensions at concentrations of 50, 100, and 200 mg·L^{-1} were utilized as seed priming agents. The sterilized seeds were soaked in these respective suspensions for 24 h, whereas the control group was soaked in distilled water. To simulate combined saline-alkali stress, mixed salt solutions containing NaCl, Na_2SO_4, Na_2CO_3, and $NaHCO_3$ were prepared at a molar ratios of 1:1:1:1, yielding final concentrations of 50, 100, and 150 mmol·L^{-1}.

For cultivation, filter papers were saturated with the prepared mixed salt solutions, while distilled water was used for the control group. The primed seeds were sown in Petri dishes lined with three layers of the saturated filter paper, with 5 g of seeds allocated per dish. The experimental design comprised a total of 16 treatments, each with three biological replicates. For daily maintenance, each Petri dish was supplemented with 5 mL of distilled water. Weekly, each dish received 5 mL of the corresponding mixed salt solution (or distilled water for the control) alongside Hoagland nutrient solution. Two weeks post-emergence, 10 mL of the respective ZnO NPs suspension was applied to each dish as a foliar spray. This foliar application was performed twice at a one-week interval. The seedlings were harvested four weeks post-emergence for subsequent experimental analysis.

2.2 Measurement of Biomass

The aboveground length (AL) of sorghum seedlings was measured using a tape measure, and the aboveground fresh weight (AFW) was determined with an electronic analytical balance. The aboveground tissues were then heated at 105°C for 30 min to deactivate enzymes, and subsequently oven-dried at 80°C for 72 h. Finally, the aboveground dry weight (ADW) was recorded using the analytical balance.

2.3 Determination of Chlorophyll Content

Chlorophyll a (Chl a) and b (Chl b) contents in sorghum leaves were determined following the methods described by Hiscox et al. [34] and Wellburn [35]. Briefly, 0.5 g of fresh leaf tissue from each treatment was cut into small segments and placed into stoppered tubes containing 10 mL of dimethyl sulfoxide (DMSO). The samples were then incubated in a water bath at 65°C for 4 h. After cooling to room temperature, the absorbance of the supernatant was measured at 645 nm and 663 nm to assess the concentrations of Chl a and Chl b, respectively.

2.4 Determination of Antioxidant Enzyme Activity

For the antioxidant enzyme assays, 0.5 g of leaf tissue was first homogenized in an ice bath at 4°C with 10 mL of pre-chilled 0.05 M phosphate buffer (PBS, pH 7.8; prepared from Na_2HPO_4 and NaH_2PO_4 and supplemented with 1% EDTA-Na_2). The homogenate was then centrifuged at 10,000 rpm for 10 min [36], and the resulting supernatant was collected and stored at 4°C for the determination of superoxide dismutase (SOD), peroxidase (POD), catalase (CAT), and ascorbate peroxidase (APX) activities. SOD activity was evaluated according to the method of Zhang et al. by measuring the inhibition of the photochemical reduction of nitroblue tetrazolium (NBT) at 560 nm [37]. POD activity was determined following the method of Samadi et al. by monitoring the oxidation rate of guaiacol at 470 nm in the presence of H_2O_2 [38]. CAT activity was assayed based on the method of Chance et al. by measuring the rate of decrease in H_2O_2 absorbance at 240 nm [39]. Finally, APX activity was assessed according to the method of Khaleghi et al. by tracking the decrease in absorbance at 290 nm resulting from the oxidation of ascorbic acid by H_2O_2 [40].

2.5 Determination of Non-Enzymatic Antioxidant Content

The ascorbic acid (AsA) content was determined following the protocol described by Huang et al. [41]. Briefly, fresh leaf samples (0.5 g) were homogenized in 5 mL of 5% PBS at 4°C. The homogenate was centrifuged at 22,000 rpm for 15 min, and the resulting supernatant was collected. AsA concentration was subsequently quantified by measuring the absorbance at 525 nm, which corresponds to the reaction product of AsA, tetraphenylbenzidine, and ferric chloride.

For the quantitative analysis of glutathione (GSH), the method established by Feng et al. was employed [42]. Leaf tissues (0.5 g) were homogenized in 5% trichloroacetic acid (TCA) at 4°C and centrifuged at 15,000 rpm for 15 min. The GSH content in the supernatant was then evaluated by monitoring the absorbance at 412 nm, reflecting the formation of a yellow compound generated from the reaction between GSH and 5,5′-dithiobis-(2-nitrobenzoic acid) (DTNB).

2.6 Determination of Lipid Peroxidation Levels

The damage of plant lipid peroxidation was evaluated by determining the malondialdehyde (MDA) content, following the protocol outlined by Tanveer et al. [43]. Briefly, 0.5 g of fresh leaf tissue was homogenized in 5 mL of 0.05 M PBS (pH 7.8) at 4°C. The homogenate was then centrifuged at 15,000 rpm

for 20 min, and the supernatant was collected. Subsequently, a 1.5 mL aliquot of the supernatant was mixed with 2.5 mL of a reaction solution containing 0.05 M PBS, 5% thiobarbituric acid (TBA), and 5% TCA. The resulting mixture was incubated in a boiling water bath (100°C) for 10 min. After cooling to room temperature, the mixture was centrifuged at 4800 rpm for 10 min. The absorbance of the final supernatant was measured at 532 nm and 600 nm to calculate the MDA content.

2.7 Determination of Na^+/K^+

The Na^+ and K^+ contents were determined following the methods described by Barin et al. [44] and Yang et al. [45]. Briefly, dried sorghum seedlings were ground into a fine powder. A 0.5 g aliquot of the powdered sample was transferred into a polytetrafluoroethylene (PTFE) tube, and 10 mL of an $HClO_4$ and HNO_3 mixture (1:4, v/v) was added for microwave digestion. After digestion, the concentrations of Na^+ and K^+ were quantified using inductively coupled plasma mass spectrometry (ICP-MS), and the Na^+/K^+ ratio was subsequently calculated.

2.8 Statistical Analysis

All experiments were performed in triplicate, and the results are expressed as the mean ± standard deviation (SD). Statistical analyses were conducted using SPSS 26.0 software. Prior to analysis, the data were assessed for normality and homogeneity of variance using the Shapiro-Wilk and Levene's tests, respectively. Once the assumptions of normal distribution and equal variances were confirmed, the data were subjected to a one-way analysis of variance (ANOVA). Subsequently, Duncan's multiple range test was employed for post hoc comparisons to identify statistically significant differences among the treatment groups ($p < 0.05$). In addition, correlation analysis was performed to evaluate the linear relationships among the various physiological indicators. Principal component analysis (PCA) was utilized for dimensionality reduction, providing a clearer visualization of the variations among different treatments. A two-way ANOVA was also conducted to determine the main effects of ZnO NPs and saline-alkali stress, as well as their interaction effects. Subsequently, response surface methodology (RSM) models were constructed using RStudio (version 2025.05.01) for an in-depth analysis of the interactive effects of ZnO NPs and saline-alkali stress on the physiological parameters, and to predict the optimal response ranges for both factors. Finally, all graphical representations were generated and processed using Origin 2025.

3 Results

3.1 Effects of ZnO NPs on the Biomass of Sorghum Seedlings under Saline-Alkali Stress

The effects of ZnO NPs on the growth of sorghum seedlings under saline-alkali stress are presented in Fig. 1. Across all treatment groups, the aboveground length of sorghum seedlings exhibited a distinct unimodal trend (initial increase followed by a subsequent decrease) with rising ZnO NPs concentrations (Fig. 1A). In the absence of saline-alkali stress, ZnO NPs at concentrations of 50–100 $mg{\cdot}L^{-1}$ significantly promoted shoot elongation, reaching a maximum of 14.5 cm (a 34.3% increase compared to the control). However, this growth was markedly inhibited by 43.4% at a concentration of 200 $mg{\cdot}L^{-1}$, suggesting a phytotoxic effect at higher dosages. Similar growth-promoting effects were observed under 50 and 100 $mmol{\cdot}L^{-1}$ saline-alkali stress, where the aboveground lengths peaked at 17.3 cm and 15 cm, respectively, at a ZnO NPs concentration of 100 $mg{\cdot}L^{-1}$, before decline at 200 $mg{\cdot}L^{-1}$.

Consistent with the changes in aboveground length, the shoot fresh weight exhibited a similar biphasic trend, rising initially before declining at higher ZnO NPs dosages (Fig. 1B). Under non-stressed conditions, the application of 50 and 100 $mg{\cdot}L^{-1}$ ZnO NPs significantly elevated the fresh weight by 24.4% and 46.2%,

respectively ($p < 0.05$). Under low to moderate saline-alkali stress (50 and 100 mmol·L^{-1}), the 100 mg·L^{-1} ZnO NPs treatment proved to be the most effective, yielding fresh weight increases of 29.6% and 24.8%, respectively. Notably, under severe stress conditions (200 mmol·L^{-1}), this same optimal concentration (100 mg·L^{-1}) demonstrated a pronounced mitigating effect, boosting the fresh weight by an impressive 61.6% compared to the control ($p < 0.05$).

Mirroring the trends observed in fresh weight, the shoot dry weight exhibited an initial increase followed by a decline as ZnO NPs concentrations rose (Fig. 1C). In the non-stressed control, the 100 mg·L^{-1} ZnO NPs treatment maximized dry weight accumulation, reaching a peak of 0.169 g (a 92.4% increase). This specific dosage (100 mg·L^{-1}) consistently provided the most pronounced growth benefits as saline-alkali stress intensified. Specifically, it enhanced dry weight by 79.3% under mild stress (50 mmol·L^{-1}), and produced striking increases of 84.0% and 208.8% under moderate to severe stress conditions (100 and 150 mmol·L^{-1}, respectively). Collectively, these growth parameters indicate that an optimal dosage of ZnO NPs (approximately 100 mg·L^{-1}) effectively alleviates saline-alkali stress and promotes sorghum seedlings growth, whereas excessive concentrations induce phytotoxicity.

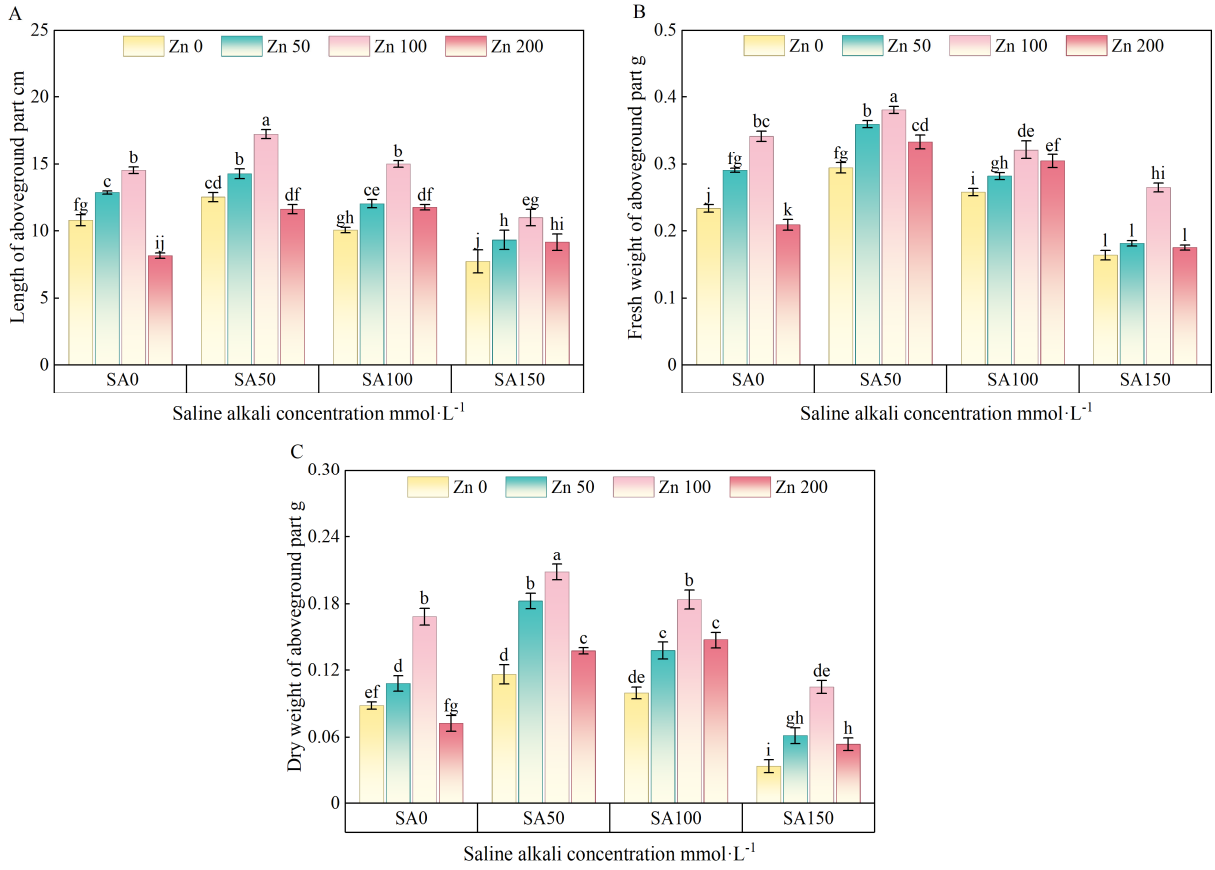

Figure 1: Effects of different concentrations of ZnO NPs and saline-alkali stress on aboveground length (**A**), aboveground fresh weight (**B**), and aboveground dry weight (**C**) of sorghum seedlings. Values represent mean ± SD ($n = 3$). Different letters indicate significant differences ($p < 0.05$).

3.2 Effects of ZnO NPs on Chlorophyll Content in Sorghum Seedlings under Saline-Alkali Stress

The effect of ZnO NPs on chlorophyll content of sorghum seedlings under saline-alkali stress is illustrated in Fig. 2. Specifically, the response of Chl a to varying ZnO NPs concentrations was highly

dependent on the severity of the stress (Fig. 2A). Under non-stressed conditions, ZnO NP application had no significant impact on Chl a levels. However, as saline-alkali stress intensified, ZnO NPs exerted a clear positive regulatory effect. Under mild stress (50 mmol·L^{-1}), the 100 and 200 mg·L^{-1} ZnO NPs treatments elevated Chl a content by 13.2% and 24.7%, respectively. As the stress escalated to 100 and 150 mmol·L^{-1}, all tested ZnO NPs concentrations significantly enhanced Chl a accumulation. Notably, the 100 mg·L^{-1} treatment yielded the most pronounced improvements, increasing Chl a content by 35.2% and 34.3% under 100 and 150 mmol·L^{-1} stress, respectively ($p < 0.05$).

The response of Chl b to ZnO NPs (Fig. 2B) presented a different pattern from that of Chl a. Under unstressed conditions, Chl b levels remained largely unaffected, with a significant alteration observed only at the highest ZnO NPs concentration (200 mg·L^{-1}). However, under mild saline-alkali stress (50 mmol·L^{-1}), the 100 mg·L^{-1} ZnO NPs treatment significantly elevated Chl b content by 47.8% ($p < 0.05$). As the stress intensified to 100 and 150 mmol·L^{-1}, Chl b accumulation exhibited a progressive increase with rising ZnO NPs concentrations. Notably, the 200 mg·L^{-1} treatment yielded the most substantial improvements, boosting Chl b by 135.8% and 92.9% under 100 and 150 mmol·L^{-1} stress, respectively ($p < 0.05$). Collectively, these findings indicate that while ZnO NPs exert minimal influence on photosynthetic pigments in the absence of stress, they significantly enhance pigment accumulation under saline-alkali conditions. Specifically, the 100 mg·L^{-1} dosage optimally promotes Chl a synthesis, whereas the 200 mg·L^{-1} concentration exerts a more pronounced stimulatory effect on Chl b ($p < 0.05$).

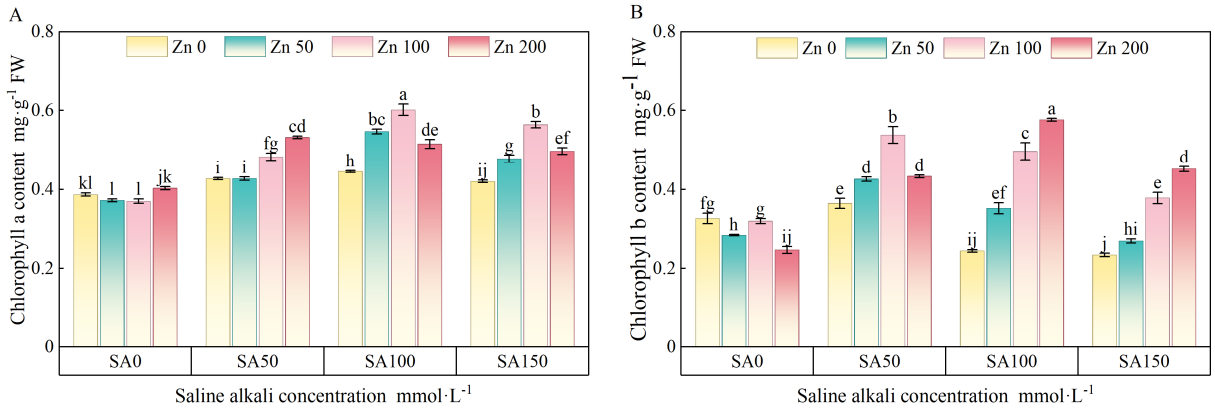

Figure 2: Effects of different concentrations of ZnO NPs and saline-alkali stress on chlorophyll a (**A**) and chlorophyll b (**B**) content in sorghum seedlings. Values represent mean ± SD ($n = 3$). Different letters indicate significant differences ($p < 0.05$).

3.3 Effects of ZnO NPs on Antioxidant Enzyme Activities in Sorghum Seedlings under Saline-Alkali Stress

The effects of ZnO NPs on the antioxidant enzyme activities of sorghum seedlings under saline-alkali stress are illustrated in Fig. 3. Overall, ZnO NPs application significantly modulated these enzyme activities across varying stress levels. In the unstressed control, the 100 mg·L^{-1} ZnO NPs treatment induced a 55.3% increase in CAT activity (Fig. 3A). Notably, this stimulatory effect intensified progressively as the severity of saline-alkali stress escalated. Compared to the respective stress controls, applying 100 mg·L^{-1} ZnO NPs dramatically enhanced CAT activity by 108.9%, 435.2%, and 449.7% under 50, 100, and 150 mmol·L^{-1} stress conditions, respectively. Similarly, ZnO NPs significantly upregulated APX activity (Fig. 3B), with the most pronounced effects observed under moderate to severe stress. Specifically, the 100 mg·L^{-1} ZnO NPs dosage

boosted APX activity by 205% and 283.1% under 100 and 150 mmol·L^{-1} saline-alkali conditions, respectively ($p < 0.05$).

POD and SOD activities corroborated the protective role of ZnO NPs. Under 50 mmol·L^{-1} saline-alkali stress, the various ZnO NPs treatments increased POD activity by 40.3%, 81.2%, and 37.1%, respectively (Fig. 3C). This upregulation was exceptionally pronounced under severe stress (150 mmol·L^{-1}), where the corresponding ZnO NPs treatments triggered striking surges in POD activity of 354.7%, 775.1%, and 522.6% ($p < 0.05$). Similarly, SOD activity was significantly enhanced (Fig. 3D). Under 50 mmol·L^{-1} stress, applications of 50 and 100 mg·L^{-1} ZnO NPs elevated SOD activity by 36.5% and 96.6%, respectively. As the stress intensified to 100 and 150 mmol·L^{-1}, the 100 mg·L^{-1} ZnO NPs dosage continued to exhibit the most potent stimulatory effect, boosting SOD activity, by 198.5% and 411.8%, respectively ($p < 0.05$). Collectively, these physiological characteristics reveal that while ZnO NPs exert no significant influence on antioxidant enzymes under non-stressed conditions, they initiate a robust, concentration-dependent defense mechanism under saline-alkali stress. Across all evaluated stress levels, the 100 mg·L^{-1} ZnO NPs dosage consistently demonstrated optimal performance in maximizing antioxidant enzyme activities.

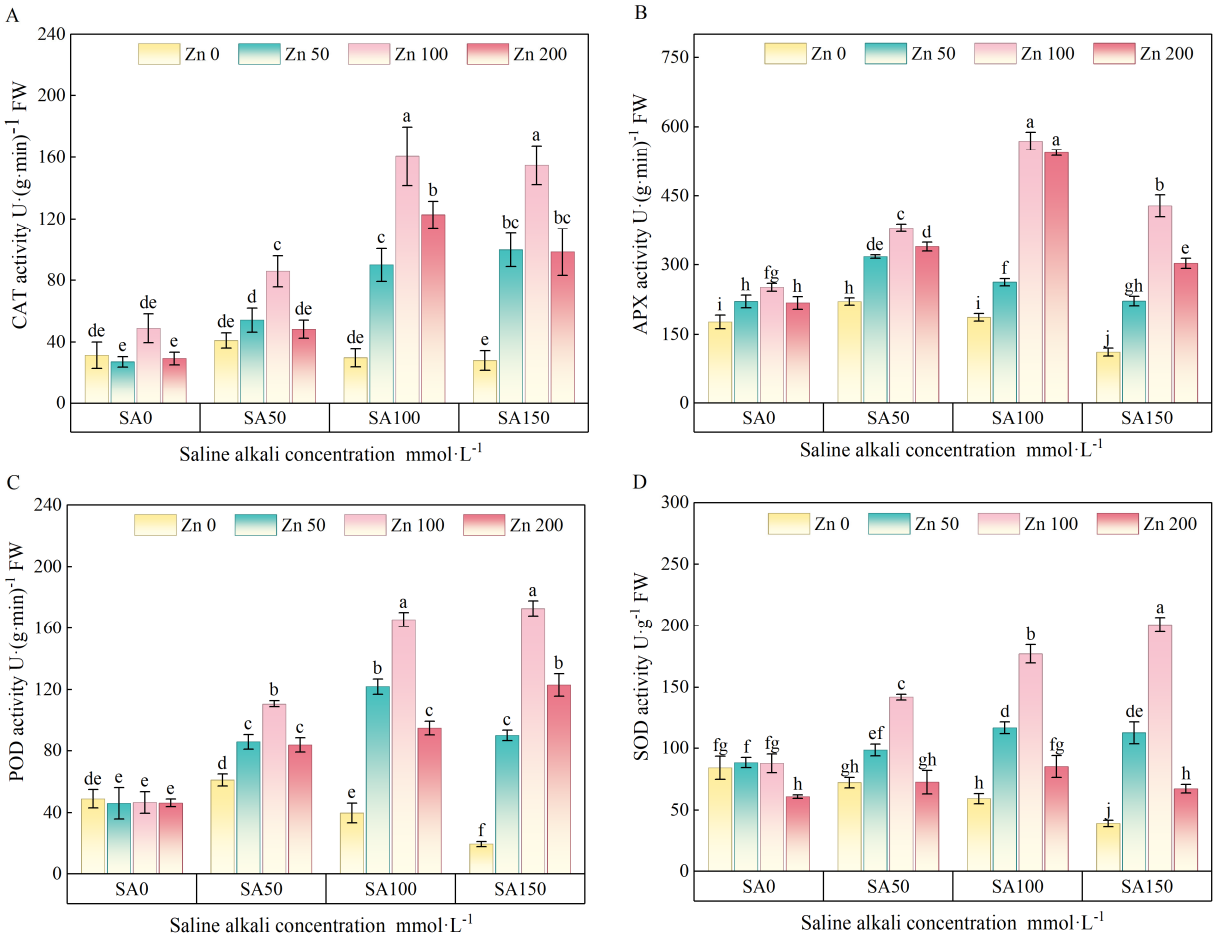

Figure 3: Effects of different concentrations of ZnO NPs and saline-alkali stress on the activities of CAT (**A**), APX (**B**), POD (**C**), and SOD (**D**) in sorghum seedlings. Values represent mean ± SD ($n = 3$). Different letters indicate significant differences ($p < 0.05$).

3.4 Effects of ZnO NPs on Non-Enzymatic Antioxidant Content in Sorghum Seedlings under Saline-Alkali Stress

The impact of ZnO NPs on the non-enzymatic antioxidant system in saline-alkali stressed sorghum seedlings is presented in Fig. 4. Mirroring the enzymatic responses, GSH content exhibited a distinct dose-dependent, biphasic trend, initially rising and subsequently declining as ZnO NPs concentrations increased (Fig. 4A). Under unstressed control conditions, the 100 mg·L^{-1} ZnO NPs treatment moderately increased GSH content by 24.6%. However, under 50 mmol·L^{-1} saline-alkali stress, this same optimal dosage (100 mg·L^{-1}) significantly boosted GSH levels by 141.3%, while the 50 and 200 mg·L^{-1} treatments also induced significant, albeit smaller, increases ($p < 0.05$). As the saline-alkali stress further intensified, the upregulatory efficacy of the 100 mg·L^{-1} treatment became increasingly pronounced, culminating in a striking 446.5% elevation in GSH content under the severe150 mmol·L^{-1} stress condition.

Regarding AsA content (Fig. 4B), the 200 mg·L^{-1} ZnO NPs treatment induced a 33.8% reduction in the unstressed control group. Conversely, under 50 mmol·L^{-1} saline-alkali stress, the application of 100 mg·L^{-1} ZnO NPs significantly elevated AsA content by 136.9% ($p < 0.05$). Under more severe saline-alkali stress conditions, all tested ZnO NPs concentrations significantly enhanced AsA accumulation, with the 100 mg·L^{-1} dosage consistently yielding the optimal response. In summary, applying an optimal dosage of ZnO NPs (100 mg·L^{-1}) ZnO NPs effectively upregulates the synthesis of critical non-enzymatic antioxidants (both GSH and ASA) to combat saline-alkali stress, whereas excessive concentrations may exert detrimental physiological effects ($p < 0.05$).

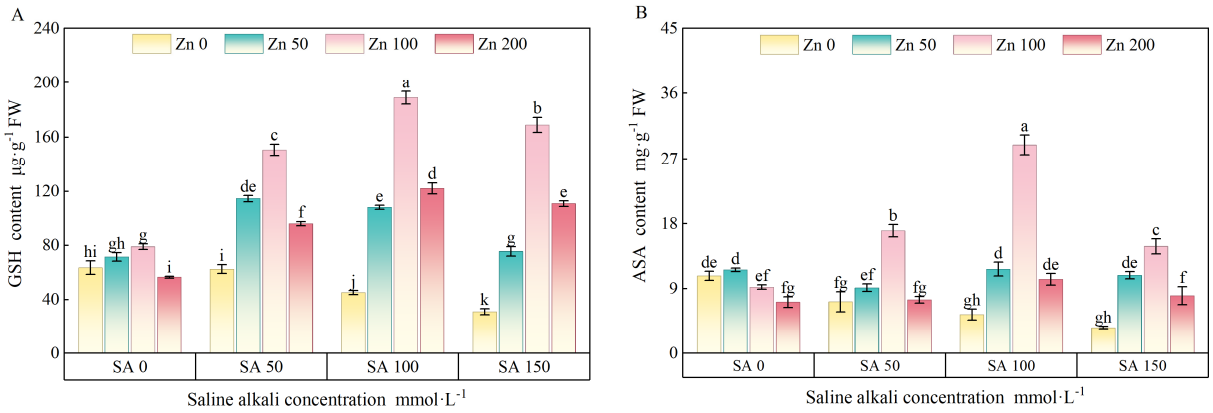

Figure 4: Effects of different concentrations of ZnO NPs and saline-alkali stress on GSH (**A**) and ASA (**B**) activities in sorghum seedlings. Values represent mean ± SD ($n = 3$). Different letters indicate significant differences ($p < 0.05$).

3.5 Effects of ZnO NPs on Na$^+$, K$^+$ and Lipid Peroxidation in Sorghum Seedlings under Saline-Alkali Stress

The effects of ZnO NPs on the Na$^+$/K$^+$ ratio and MDA content in sorghum seedlings under saline-alkali stress are presented in Fig. 5. In the non-stressed control group, ZnO NPs treatments did not significantly alter the Na$^+$/K$^+$ ratio (Fig. 5A), which remained stable at approximately 1 across all applied concentrations. However, as the severity of saline-alkali stress intensified, notable changes were observed, with ZnO NPs applications leading to a profound and significant reduction in the Na$^+$/K$^+$ ratio ($p < 0.05$). Specifically, under 50 mmol·L^{-1} saline-alkali stress, the application of 100 mg·L^{-1} ZnO NPs resulted in a striking 96.9% decrease in this ratio. This potent mitigating effect persisted at higher stress levels, where the same

100 mg·L^{-1} dosage reduced the Na^+/K^+ ratio by 90.4% and 97.1% under 100 and 150 mmol·L^{-1} saline-alkali stress, respectively.

MDA serves as a critical marker for lipid peroxidation, reflecting the extent of cell membrane damage. Under non-stressed control conditions, the highest concentration of ZnO NPs (200 mg·L^{-1}) induced a significant 74.7% increase in MDA content (Fig. 5B). Conversely, under 50 mmol·L^{-1} saline-alkali stress, the 100 mg·L^{-1} ZnO NPs application significantly decreased MDA levels by 46.3%, whereas the 200 mg·L^{-1} treatment caused a slight, yet significant, accumulation of MDA ($p < 0.05$). As the severity of saline-alkali stress escalated to 100 and 150 mmol·L^{-1}, treatments with 50 and 100 mg·L^{-1} ZnO NPs markedly alleviated MDA accumulation. Most notably, under the severe 150 mmol·L^{-1} stress condition, the 100 mg·L^{-1} dosage achieved a striking 85.2% reduction in MDA levels ($p < 0.05$). Collectively, these findings elucidate the physiological mechanisms by which appropriate ZnO NPs application (optimally at 100 mg·L^{-1}) mitigates saline-alkali-induced oxidative damage in sorghum seedlings, while demonstrating that excessive concentrations can act as a pro-oxidant, exacerbating membrane injury.

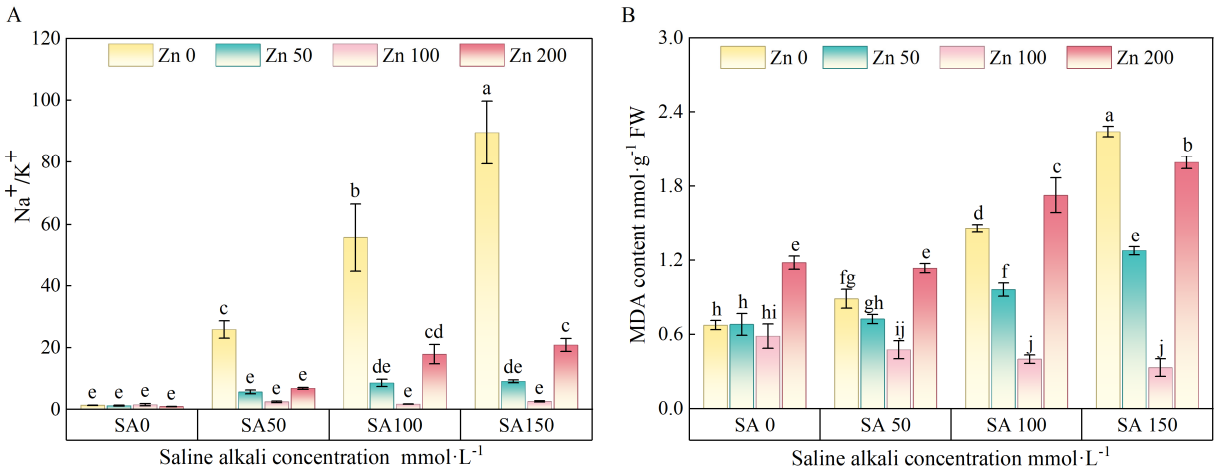

Figure 5: Effects of different concentrations of ZnO NPs and saline-alkali stress on Na^+/K^+ (**A**) and MDA (**B**) contents in sorghum seedlings. Values represent mean ± SD ($n = 3$). Different letters indicate significant differences ($p < 0.05$).

3.6 Correlation Analysis

The Pearson correlation heatmap (Fig. 6) reveals significant physiological interrelationships in ZnO NPs-treated sorghum seedlings under saline-alkali stress. A pronounced synergistic network was identified among growth traits, photosynthetic pigments, and antioxidants. Growth indicators (AL, AFW, ADW) were strongly positively intercorrelated ($r \geq 0.91$, $p \leq 0.001$). Moreover, robust links emerged between photosynthetic pigments and antioxidant enzymes, notably Chl a with CAT/POD ($r = 0.84/0.87$) and Chl b with APX ($r = 0.85$). The antioxidant system displayed highly synchronized directional changes ($p \leq 0.001$), evidenced by strong correlations among enzymes (e.g., CAT vs. POD, $r = 0.92$) and between enzymatic and non-enzymatic components (e.g., POD vs. GSH, $r = 0.93$; SOD vs. AsA, $r = 0.83$).

In contrast, stress markers displayed clear inverse relationships with plant health indicators. MDA negatively correlated with growth traits (AL, AFW, ADW; $r = -0.65$ to -0.71, $p \leq 0.01$) and antioxidants (GSH, AsA; $r = -0.50$, -0.62, $p \leq 0.05$). Concurrently, the Na^+/K^+ ratio exhibited negative correlations with AL, SOD, GSH, and AsA ($p \leq 0.05$). Importantly, the Na^+/K^+ ratio correlated positively and strongly with MDA ($r = 0.73$, $p \leq 0.01$). Together, these results demonstrate that elevated oxidative stress and

disrupted ion homeostasis are consistently associated with diminished seedling growth and impaired antioxidant defenses.

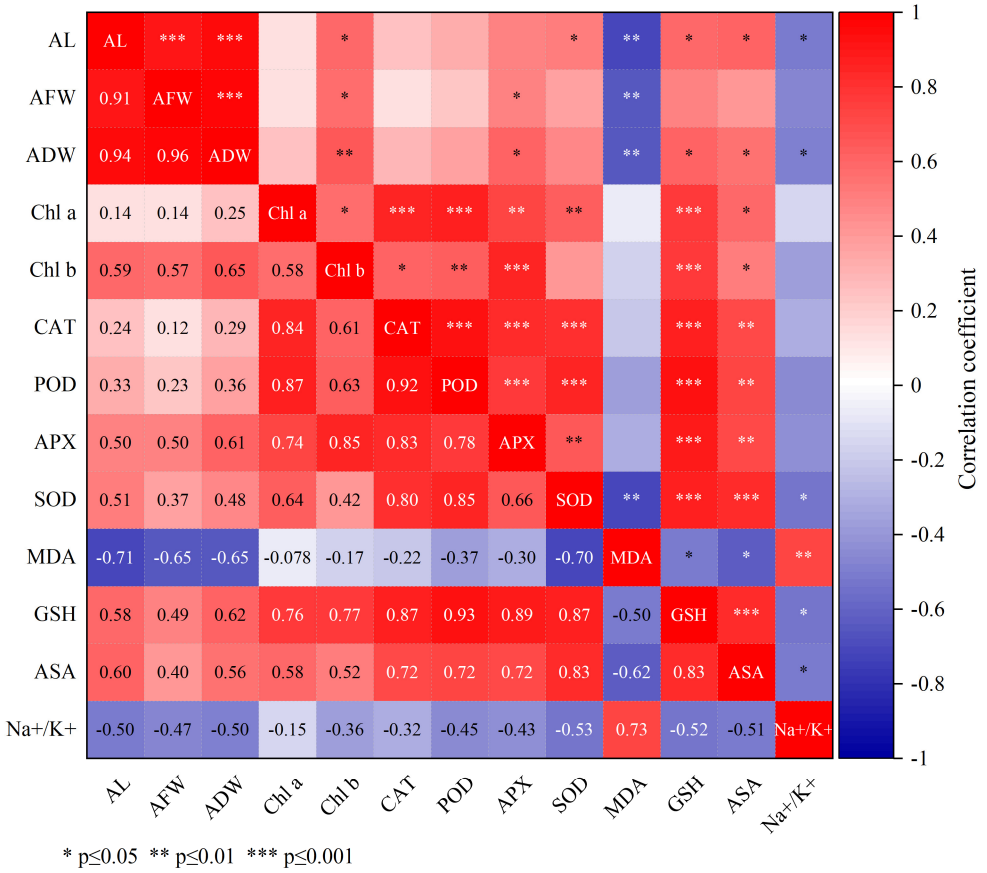

Figure 6: Pearson correlation analysis of various growth and physiological parameters in sorghum seedlings under ZnO NPs treatment. *, **, and *** indicate significant correlations at $p \leq 0.05$, $p \leq 0.01$, and $p \leq 0.001$, respectively.

3.7 Principal Component Analysis

To comprehensively evaluate the physiological response patterns of sorghum seedlings to saline-alkali stress under varying ZnO NPs treatments, a principal component analysis (PCA) was performed on the 13 evaluated physiological indicators (Table 1). Two principal components with eigenvalues greater than 1 were extracted (12.6933 and 4.0538, respectively). The first (PC1) and second (PC2) principal components accounted for 60.4% and 19.3% of the total variance, respectively. Together, they yielded a cumulative variance contribution of 79.7%, effectively capturing the majority of the dataset's variability and satisfying the analytical requirements for dimensionality reduction. An analysis of the variable loadings revealed that PC1 was primarily driven by Chlb, APX, SOD, GSH, AsA, and the Na^+/K^+ ratio. Conversely, PC2 was largely dominated by the growth indices (AL, AFW and ADW), along with Chla, CAT, POD, and MDA.

Subsequently, a comprehensive evaluation score (F) was calculated for each treatment by weighing the principal component score (F_1 and F_2) against their respective variance contribution ($F = F_1 \times 60.4\% + F_2 \times 19.3\%$). All treatments were then ranked according to their resulting F values (Table 2). The analysis revealed that ZnO NPs applications generally improved the overall rankings of sorghum seedlings under saline-alkali stress. Most notably, the top three positions were exclusively occupied by the 100 $mg{\cdot}L^{-1}$ ZnO NPs treatments. This quantitative assessment not only substantiates the positive regulatory role of ZnO

NPs in promoting seedling growth but also confirms the 100 mg·L^{-1} dosage as the optimal concentration for maximizing multidimensional physiological resilience. Furthermore, these comprehensive rankings are in perfect alignment with the empirical observations of seedling growth and physiological responses detailed above.

Table 1: Principal component analysis and variance interpretation.

Index	Load	
	PC1	PC2
AL	0.2223	−0.2643
AFW	0.2003	−0.2986
ADW	0.2293	−0.2453
Chla	0.1759	0.3316
Chlb	0.2098	0.0627
CAT	0.2045	0.3126
POD	0.2245	0.2761
APX	0.2367	0.1410
SOD	0.2382	0.1301
MDA	−0.1948	0.2149
GSH	0.2642	0.1519
ASA	0.2402	0.0721
Na^+/K^+	−0.1785	0.1239
Eigen values	12.6933	4.0538
Proportion of variance/%	60.4445	19.3036
Cumulative variance/%	60.4445	79.7481

Note: PC1 and PC2 represent principal component 1 and principal component 2, respectively. The same as below.

Table 2: Comprehensive score and ranking of physiological effects of ZnO-NPs treatment on sorghum seedlings.

Treatment	Principal Component Score		Comprehensive Score	Comprehensive Score Ranking
	F_1 (PC1)	F_2 (PC2)		
SA 0 Zn 0	−0.5586	−0.5536	−0.4445	13
SA 0 Zn 50	−0.3116	−1.0762	−0.3961	12
SA 0 Zn 100	0.1270	−1.8387	−0.2782	10
SA 0 Zn 200	−0.9311	−0.2782	−0.6165	14
SA 50 Zn 0	−0.4520	−0.6007	−0.3892	11
SA 50 Zn 50	0.5274	−0.9963	0.1265	6
SA 50 Zn 100	1.5168	−0.9023	0.7426	3
SA 50 Zn 200	0.1176	−0.1369	0.0447	7
SA 100 Zn 0	−1.0324	−0.2076	−0.6641	15
SA 100 Zn 50	0.3493	0.2658	0.2624	5
SA 100 Zn 100	2.0706	0.7628	1.3988	1
SA 100 Zn 200	0.4092	0.5278	0.3492	4
SA 150 Zn 0	−1.8946	−0.7882	−1.2973	16
SA 150 Zn 50	−0.5216	0.9824	−0.1256	9
SA 150 Zn 100	1.0779	1.5800	0.9565	2
SA 150 Zn 200	−0.4938	1.6834	0.0265	8

3.8 Response Surface Analysis

To comprehensively evaluate the coupling effects between ZnO NPs and saline-alkali stress, a RSM was applied to the 13 evaluated growth and physiological indices (Table 3). An initial two-way ANOVA (Table 4)

revealed that the individual main effects of ZnO NPs and saline-alkali stress, as well as their interaction, exerted a highly significant influence on all tested parameters ($p < 0.001$). Three-dimensional response surface plots illustrating these interactive effects on AL, APX, MDA, and the Na^+/K^+ ratio are presented in Fig. 7. Based on the model optimization, the beneficial indicators AL and APX achieved their theoretical maximum at the coordinate points (ZnO NPs concentration, saline-alkali concentration) of (111.33, 77.84) and (105.04, 95.56), respectively. Conversely, the stress markers MDA and the Na^+/K^+ ratio were minimized at the coordinates (89.65, 50.32) and (98.16, 64.87), respectively.

Finally, by integrating these predictive models to map the combined distribution surface, an optimal overlapping parameter region was identified (Fig. 8). This rectangular region is bounded by a ZnO NPs range of 89.65–118.53 $mg{\cdot}L^{-1}$ and a saline-alkali stress range of 50.04–96.56 $mmol{\cdot}L^{-1}$. Consequently, the optimal application range of ZnO NPs for mitigating saline-alkali stress was mathematically pinpointed to 89.65–118.53 $mg{\cdot}L^{-1}$. Notably, this theoretically derived optimal range perfectly aligns with the empirical phenotypic and physiological observations detailed previously.

Table 3: Response surface analysis of sorghum seedling growth and physiological indexes to ZnO NPs and saline alkali stress.

Index	Factor	For Factors		Total Model			
		F Value	Pr > F	F Value	Pr > F	Critical Value	Stationary Point
AL	ZnO NPs	28.22	<0.001	61.50	<0.001	111.33	Maximum
	SA	186.65	<0.001	R^2 = 0.9361		77.84	16.81
AFW	ZnO NPs	19.38	<0.001	67.44	<0.001	115.18	Maximum
	SA	272.28	<0.001	R^2 = 0.9414		50.04	0.41
ADW	ZnO NPs	28.52	<0.001	109.50	<0.001	108.67	Maximum
	SA	385.33	<0.001	R^2 = 0.9630		59.17	0.21
Chla	ZnO NPs	24.29	<0.001	13.99	<0.001	174.31	Maximum
	SA	10.74	0.004	R^2 = 0.7691		104.73	0.60
Chlb	ZnO NPs	70.40	<0.001	31.27	<0.001	103.43	Maximum
	SA	48.49	<0.001	R^2 = 0.8816		87.94	0.56
CAT	ZnO NPs	35.33	<0.001	25.77	<0.001	96.77	Maximum
	SA	46.72	<0.001	R^2 = 0.8599		120.02	169.83
POD	ZnO NPs	36.18	<0.001	20.27	<0.001	116.67	Maximum
	SA	19.76	<0.001	R^2 = 0.8284		78.16	172.30
APX	ZnO NPs	47.34	<0.001	35.05	<0.001	105.04	Maximum
	SA	101.50	<0.001	R^2 = 0.8626		95.56	590.45
SOD	ZnO NPs	47.48	<0.001	23.07	<0.001	118.53	Maximum
	SA	15.35	<0.001	R^2 = 0.8267		86.71	187.91
MDA	ZnO NPs	11.77	0.002	40.85	<0.001	89.65	Minimum
	SA	15.28	<0.001	R^2 = 0.9068		50.32	0.64
GSH	ZnO NPs	169.60	<0.001	60.22	<0.001	166.47	Maximum
	SA	2.13	0.159	R^2 = 0.9348		100.79	193.18
ASA	ZnO NPs	27.92	<0.001	19.72	<0.001	107.75	Maximum
	SA	0.0033	0.955	R^2 = 0.8244		100.05	25.10
Na^+/K^+	ZnO NPs	5.11	0.034	37.05	<0.001	98.16	Minimum
	SA	15.46	<0.001	R^2 = 0.8982		64.87	4.13

Table 4: Effects of ZnO NPs and saline alkali stress and their interaction on growth and physiological indexes of Sorghum Seedlings.

	ZnO NPs		SA		ZnO NPs* SA		Modified Model		R^2
	F Value	Pr > F	F Value	Pr > F	F Value	Pr > F	F Value	Pr > F	
AL	99.60	<0.001	159.84	<0.001	10.20	<0.001	69.96	<0.001	0.969
AFW	82.06	<0.001	579.14	<0.001	16.23	<0.001	173.41	<0.001	0.987
ADW	99.34	<0.001	395.11	<0.001	8.90	<0.001	128.06	<0.001	0.983
Chla	82.57	<0.001	105.43	<0.001	44.63	<0.001	69.32	<0.001	0.969
Chlb	213.98	<0.001	136.20	<0.001	51.53	<0.001	113.31	<0.001	0.981
CAT	34.20	<0.001	49.13	<0.001	2.29	0.100	21.98	<0.001	0.907
POD	222.70	<0.001	107.43	<0.001	34.14	<0.001	99.61	<0.001	0.978
APX	363.80	<0.001	211.01	<0.001	76.88	<0.001	182.14	<0.001	0.988
SOD	336.32	<0.001	22.15	<0.001	12.55	<0.001	153.57	<0.001	0.977
MDA	492.33	<0.001	59.90	<0.001	31.02	<0.001	95.89	<0.001	0.986
GSH	682.17	<0.001	65.43	<0.001	44.27	<0.001	209.03	<0.001	0.989
ASA	280.75	<0.001	79.26	<0.001	33.86	<0.001	106.93	<0.001	0.979
Na^+/K^+	140.50	<0.001	31.33	<0.001	16.95	<0.001	51.43	<0.001	0.958

Note: * indicates the interaction between ZnO NPs and SA.

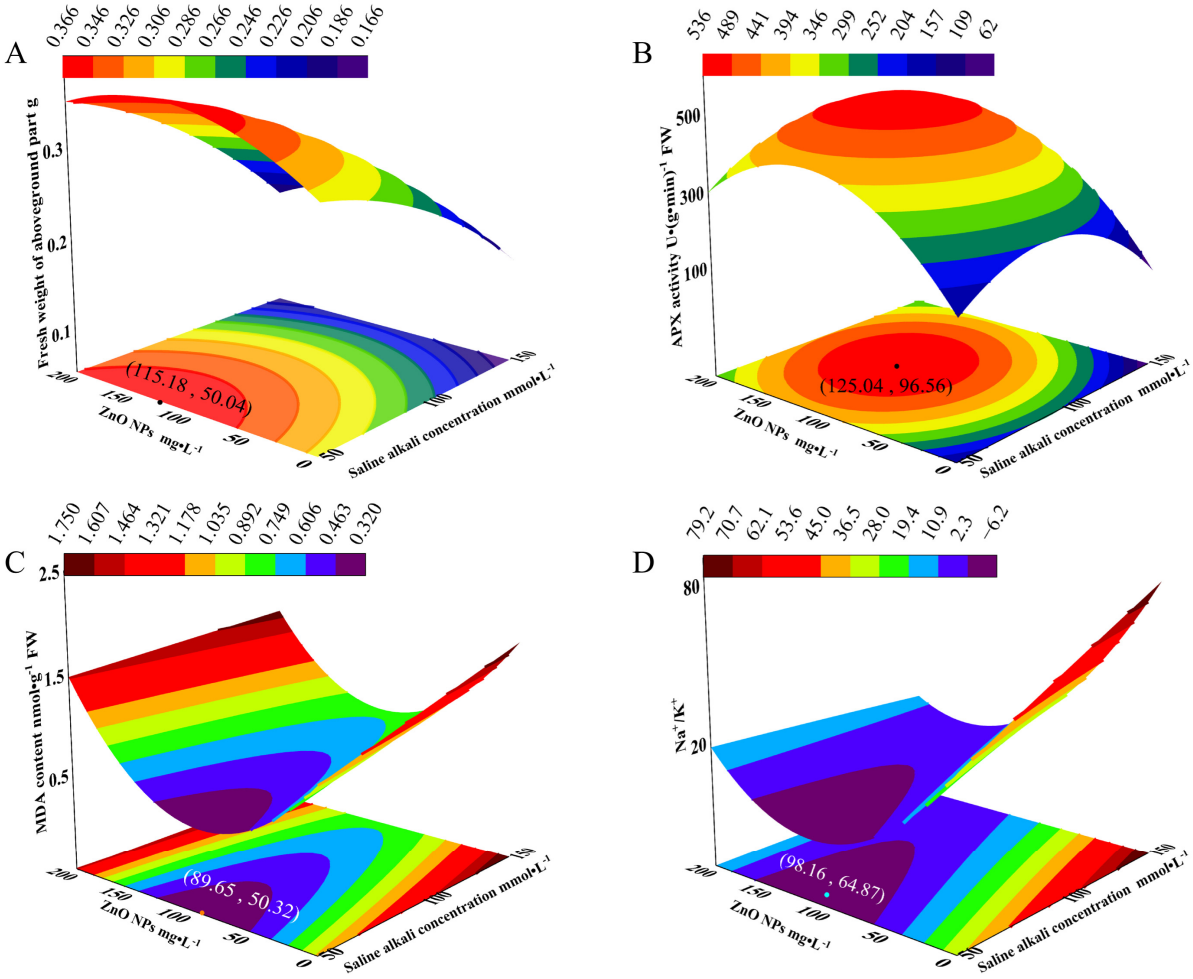

Figure 7: Response surface plots showing the interactive effects of ZnO NPs and saline-alkali stress on AFW (**A**), APX (**B**), MDA (**C**), and Na^+/K^+ (**D**) in sorghum seedlings.

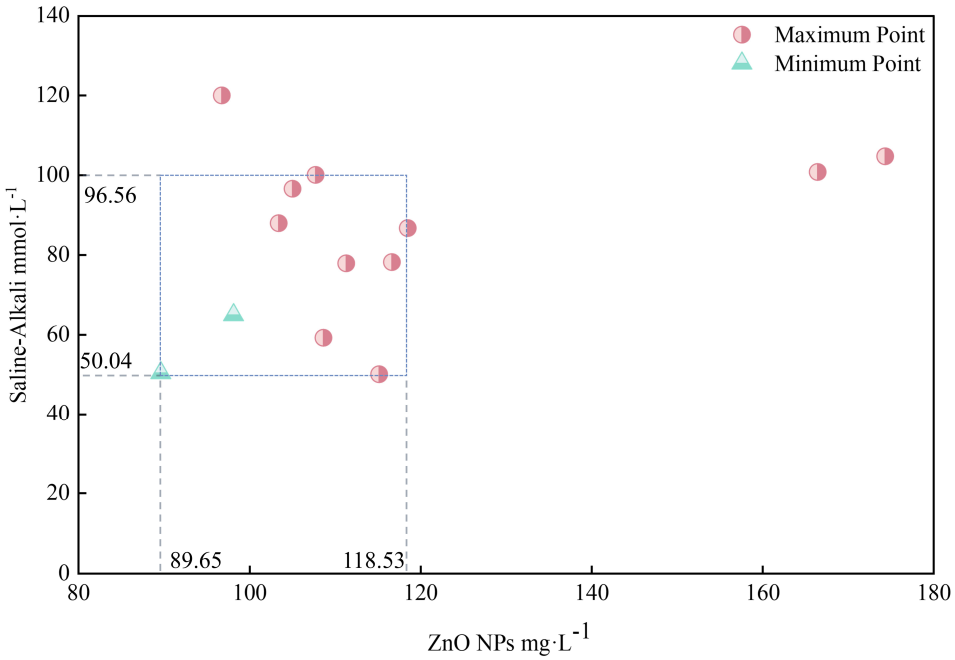

Figure 8: Distribution surface of effects of ZnO NPs and saline alkali stress on growth and physiological indexes of Sorghum Seedlings.

4 Discussion

Excessive saline-alkali stress induces severe osmotic stress and ion toxicity, which fundamentally inhibit plant growth and reduce biomass accumulation. Furthermore, it disrupts ion homeostasis by increasing tissue Na^+ content and decreasing K^+ content, exacerbates peroxidative damage to cell membranes, and suppresses photosynthesis, particularly under high pH conditions [46]. Therefore, this study systematically investigates the individual and combined effects of varying concentrations of ZnO NPs and saline-alkali stress on the growth and physiological characteristics of sorghum seedlings. Ultimately, this research elucidates the crucial role of ZnO NPs in alleviating saline-alkali-induced oxidative damage, ion imbalance, and photosynthetic inhibition.

The results of this study indicate that saline-alkali stress significantly inhibited the plant height, as well as the dry and fresh weights, of sorghum seedlings (Fig. 1). This inhibition is attributed not only to the osmotic stress and ion toxicity induced by elevated Na^+ concentrations but also, and perhaps more importantly, to the high pH. The elevated pH likely disrupts the integrity of root epidermal cells and causes the precipitation and inactivation of crucial metal ions in the rhizosphere microenvironment, thereby exacerbating nutrient deficiency [7]. However, the exogenous application of ZnO NPs significantly reversed this growth inhibition, exhibiting a typical hormetic effect (i.e., promotion at low concentrations and inhibition at high concentrations). Among the treatments, the 100 $mg{\cdot}L^{-1}$ ZnO NPs application yielded the optimal mitigating effect. This is consistent with the findings of Iftikhar and Shah regarding the response of maize to alkali stress. They noted that moderate doses of nano-Zn can penetrate cell walls more efficiently and act as a slow-release source of the trace element Zn, which activates auxin biosynthesis and the activities of enzymes associated with cell division, thereby promoting seedling morphogenesis [47]. Compared with traditional zinc fertilizers, the high specific surface area and unique physicochemical properties of ZnO NPs render them more stable in alkaline soil solutions and less prone to forming zinc hydroxide precipitates.

This enhanced stability is likely the key reason why ZnO NPs can effectively promote sorghum growth under saline-alkaline conditions [48].

Photosynthesis is central to plant energy metabolism and is among the physiological processes most susceptible to saline-alkali stress. Its inhibition primarily stems from stomatal limitations, the degradation of photosynthetic pigments, and damage to the Photosystem II (PSII) reaction center [49]. Under high pH conditions, the membrane system sustains more severe damage, resulting in an accelerated degradation of these pigments. In the present study, ZnO NPs treatments increased Chl a and b contents by up to 35.2% and 135.8%, respectively (Fig. 2). These results align with the findings of Seleiman et al., who reported that the exogenous application of ZnO NPs to salt-stressed maize not only significantly increased the relative chlorophyll content (SPAD) by 42%, but also enhanced the maximum photochemical efficiency (Fv/Fm) by 29%, thereby effectively mitigating photoinhibition caused by excess light energy [50]. Additionally, recent research by Zhai et al. on the apple rootstock M9-T337 demonstrated that ZnO NPs can upregulate the expression of chlorophyll biosynthesis genes (such as ChlH and CAO) while concurrently inhibiting chlorophyll degradation. Furthermore, ZnO NPs enhance the plant's uptake of essential nutrients associated with photosynthetic pigment synthesis and photosystem functionality, such as Mg and Fe. This promotes chlorophyll synthesis and, consequently, maintains the overall integrity of the photosynthetic apparatus [51].

Saline-alkali stress induces an excessive accumulation of reactive oxygen species (ROS), leading to membrane lipid peroxidation and cellular structural damage, particularly under high pH conditions [17,52]. The antioxidant enzyme system serves as the primary line of defense for plants to scavenge excess ROS and maintain cellular redox homeostasis; thus, the magnitude of these enzyme activities directly reflects the plant's capacity for self-protection under stress. The present study demonstrates that ZnO NPs treatments significantly enhanced the activities of SOD, CAT, POD, and APX (Fig. 3), thereby substantially reducing MDA levels (Fig. 5B). These findings align with the research by Faizan et al., on tomatoes, which showed that the exogenous application of ZnO NPs under salt stress significantly increased SOD, CAT, and APX activities while simultaneously decreasing H_2O_2 and MDA contents [15]. However, the mechanism by which ZnO NPs elevate antioxidant capacity is not limited solely to their role as a nutritional supplement (i.e., serving as an enzyme cofactor). A more profound underlying reason likely involves their activation of plant stress signal transduction networks.

ZnO NPs may act as an elicitor to activate the defense system by regulating the ROS signaling pathway. Although excessive ROS lead to cytotoxicity, low concentrations of ROS serve as crucial signaling molecules within plants. As indicated by Dumanović et al., ROS can function as second messengers that are perceived by receptor kinases on the cell membrane, subsequently activating the mitogen-activated protein kinase (MAPK) cascade [53]. In the present study, the exogenous application of ZnO NPs likely induced the localized production of trace amounts of ROS within the cells. This transient ROS fluctuation signal upregulated the transcription levels of antioxidant enzyme genes, thereby triggering a systemic antioxidant defense response [16]. This mechanism is corroborated at the molecular level by Qian et al., who found that ZnO NPs treatments significantly upregulated the expression of genes associated with the MAPK cascade and antioxidant systems in cotton, thereby enhancing the plant's adaptability to saline-alkali stress [54]. Furthermore, the enhancement of the antioxidant system is closely linked to osmotic regulation mechanisms. Saline-alkali stress causes water loss in plant cells, whereas ZnO NPs maintain cell turgor by promoting the accumulation of osmoprotectants. The elevated enzyme activities observed in this study help preserve cell membrane integrity, creating a stable environment for the intracellular accumulation of solutes. In a related study on sorghum, Rakgotho et al. reported that ZnO NPs treatments significantly increased the contents of proline and soluble sugars in the leaves. These organic solutes not only act as osmolytes to

lower the cellular water potential but also stabilize the structures of biological macromolecules, working synergistically with antioxidant enzymes to scavenge free radicals [48].

In this study, a significant elevation in the key components of the ascorbate-glutathione (AsA-GSH) cycle was observed (Fig. 4), representing the primary pathway for H_2O_2 scavenging in plants. The enhanced efficiency of this cycle operates synergistically with the antioxidant enzyme system to maintain intracellular redox homeostasis, thereby effectively mitigating MDA accumulation and preserving membrane integrity [55]. Furthermore, correlation analysis indicated that growth indices were significantly and positively correlated with both antioxidant enzyme activities and non-enzymatic antioxidant levels, whereas they exhibited significant negative correlations with MDA levels and the Na^+/K^+ ratio. Additionally, a positive correlation was noted between MDA levels and the Na^+/K^+ ratio (Fig. 6). Collectively, these findings suggest that ZnO NPs promote sorghum growth under saline-alkali stress by bolstering antioxidant capacity, alleviating membrane lipid peroxidation, and maintaining intracellular ion homeostasis."

Maintaining a low cytosolic Na^+/K^+ ratio is a fundamental mechanism of plant salt-alkali tolerance. In this study, treatment with ZnO NPs significantly reduced Na^+ accumulation and increased K^+ levels in sorghum seedlings (Fig. 5A). This finding aligns with the research of Qian et al. on cotton (*Gossypium hirsutum*), which demonstrated that ZnO NPs induce the expression of the plasma membrane Na^+/H^+ antiporter (SOS1) gene. This upregulation promotes Na^+ efflux while concurrently restricting passive Na^+ influx via non-selective cation channels (NSCCs) [54]. Under high pH conditions, plant roots demand substantial ATP expenditure to maintain the transmembrane proton gradients necessary for Na^+ exclusion. ZnO NPs may enhance the activity of the plasma membrane proton pump (H^+-ATPase), thereby augmenting the driving force for ion homeostasis without excessively depleting metabolic energy reserves [56]. Furthermore, Türkoğlu et al. reported that in quinoa (*Chenopodium quinoa*), ZnO NPs sustain cell membrane selective permeability by promoting Ca^{2+} uptake in roots. This is particularly relevant because Ca^{2+}, a critical secondary messenger in the SOS signaling pathway, competitively inhibits Na^+ binding sites [57]. Consequently, the significant reduction in the Na^+/K^+ ratio observed in our study suggests that ZnO NPs function not merely as nutritional supplements, but actively operate as regulators of ion transport signaling.

The seedling stage represents a critical phase for the vegetative development of plants. During this period, the root system is not yet fully established, and both the ion exclusion barriers and transport systems remain functionally immature. Consequently, the initial development of roots and leaves directly dictates the plant's subsequent growth trajectory and yield potential. Moreover, seedlings exhibit heightened sensitivity to environmental stress, which can severely inhibit cell division and constrain biomass accumulation. The exogenous application of ZnO NPs during this vulnerable window bolsters the antioxidant defense system by enhancing the activities of key enzymes (SOD, POD, CAT, and APX) and increasing the levels of non-enzymatic antioxidants (ASA and GSH). This coordinated response mitigates oxidative damage, as evidenced by reduced MDA accumulation. Concurrently, ZnO NPs protect the photosynthetic apparatus by sustaining Chl a and b contents, thereby ensuring continuous carbon assimilation and energy supply for robust root and shoot morphogenesis [58]. The results of our study on sorghum seedlings effectively substantiate this early-stage protective mechanism.

In this study, a distinct dual concentration effect of ZnO NPs on sorghum seedlings was observed, classically characterized as a hormetic (biphasic) response. Moderate concentrations (50–100 $mg{\cdot}L^{-1}$) of ZnO NPs exerted significant beneficial effects, whereas excessive concentrations (200 $mg{\cdot}L^{-1}$) led to declines in growth parameters and elevated MDA content, indicative of pronounced phytotoxicity. This aligns with research by Ahmed et al., which revealed that high doses of metal oxide nanoparticles can trigger "nano-specific" oxidative stress. This stress generates ROS at levels that overwhelm the plant's

antioxidant defense capacity, ultimately inducing programmed cell death [59]. Therefore, the precise regulation of ZnO NPs application rates is imperative for agricultural practices. Our findings suggest that the optimal concentration is approximately 100 mg·L^{-1}, establishing a valuable reference dosage for leveraging nanotechnology to mitigate saline-alkali stress in sorghum cultivated in semi-arid regions.

Although this study elucidates the physiological mechanisms underlying the ZnO NPs-mediated alleviation of saline-alkali stress in sorghum, significant differences in physicochemical properties exist between hydroponic environments and real soil ecosystems. In practical agricultural applications, the environmental safety of ZnO NPs and their interactions with complex soil matrices must not be overlooked. Research by Strekalovskaya et al. demonstrated that while appropriate concentrations of ZnO NPs can promote plant growth and enhance stress resilience, their excessive accumulation in soil may exert toxic effects on soil microbial communities. This accumulation can inhibit the colonization and enzymatic activities of beneficial microorganisms, and even disrupt key ecological processes such as the nitrogen cycle [60]. Furthermore, Shah et al. confirmed that soil texture mediates nanoparticle toxicity, revealing significant differences in the degree to which ZnO NPs inhibit microbial respiration and community activity across various soil types [61]. Notably, a recent study by Markowicz et al. discovered that exposure to ZnO NPs in soil environments may even facilitate the horizontal transfer of antibiotic resistance genes within soil microbial communities, thereby posing a potential threat to the health of agricultural ecosystems [62]. Therefore, a comprehensive evaluation of application dosages and associated environmental factors is imperative before scaling up the use of ZnO NPs for the amelioration of saline-alkali soils in field-grown sorghum.

5 Conclusion

In conclusion, the exogenous application of ZnO NPs at appropriate concentrations serves as a highly effective strategy for mitigating saline-alkali stress in sorghum seedlings. Mechanistically, ZnO NPs promote aboveground growth by providing essential Zn nutrition. Furthermore, they sustain metabolic activity by stabilizing photosynthetic pigments and restoring intracellular Na^+/K^+ homeostasis. Crucially, ZnO NPs effectively scavenge ROS by upregulating enzymatic antioxidants (e.g., SOD and CAT) and activating the non-enzymatic ascorbate-glutathione (AsA-GSH) cycle. These coordinated responses preserve cell membrane integrity, ultimately alleviating stress-induced damage. Supported by PCA and RSM, our findings establish that the optimal ZnO NPs concentration for stress mitigation is approximately 100 mg·L^{-1}. However, caution must be exercised, as supra-optimal concentrations can induce phytotoxicity, leading to growth inhibition and exacerbated oxidative stress.

Despite these promising findings, we acknowledge certain limitations in the present study. Primarily, the experiments were conducted using a hydroponic system, which may not fully replicate the complex physicochemical interactions present in natural soil environments. Therefore, the environmental behavior and potential ecological risks of these nanomaterials warrant further evaluation. Future research should prioritize field trials to validate the efficacy and stability of ZnO NPs in actual saline-alkali soils. Concurrently, multi-omics approaches (such as transcriptomics and metabolomics) should be employed to thoroughly elucidate the molecular pathways and key genes regulatory networks underlying ZnO NPs-mediated stress tolerance in sorghum. Finally, assessing the long-term impacts of ZnO NPs application on soil microbial community structures and overall ecological safety is imperative for advancing the sustainable development of nano-agricultural technologies.

Acknowledgement: Thank you to Jin Lishan and Huo Rong for their assistance.

Funding Statement: This research was supported by the Inner Mongolia Natural Science Foundation (2024LHMS03038), the Inner Mongolia Autonomous Region Innovation Start-up Support Program for Returning Overseas Scholars, and the Specialized-Innovation Integration Course Development Project of Inner Mongolia University of Technology (ZC2023041).

Author Contributions: The authors confirm contribution to the paper as follows: Conceptualization, Haoran Li and Qi Sun; methodology, Haoran Li, Qi Sun and Haoran Sun; validation, Haoran Li, Ziyan Wu and Wenjin Wang; formal analysis, Haoran Li and Qi Sun; investigation, Haoran Li and Haoran Sun; resources, Haoran Li and Ziyan Wu; data curation, Haoran Li and Wenjin Wang; writing—original draft preparation, Haoran Li; writing—review and editing, Fang Liu; visualization, Haoran Li; supervision, Fang Liu, Haoran Li, Ziyan Wu and Wenjin Wang; project administration, Haoran Li, Ziyan Wu and Wenjin Wang; funding acquisition, Fang Liu. All authors reviewed and approved the final version of the manuscript.

Availability of Data and Materials: The data that support the findings of this study are available from the corresponding author, Fang Liu, upon reasonable request.".

Ethics Approval: Not applicable.

Conflicts of Interest: The authors declare no conflicts of interest.

References

1. Singh A. Soil salinity: a global threat to sustainable development. Soil Use Manag. 2022;38(1):39–67. [CrossRef].
2. Hassani A, Azapagic A, Shokri N. Global predictions of primary soil salinization under changing climate in the 21st century. Nat Commun. 2021;12(1):6663. [CrossRef].
3. Metternicht GI, Zinck JA. Remote sensing of soil salinity: potentials and constraints. Remote Sens Environ. 2003;85(1):1–20. [CrossRef].
4. Yu J, Chen S, Wang T, Sun G, Dai S. Comparative proteomic analysis of *Puccinellia tenuiflora* leaves under Na_2CO_3 stress. Int J Mol Sci. 2013;14(1):1740–62. [CrossRef].
5. Sun J, He L, Li T. Response of seedling growth and physiology of Sorghum bicolor (L.) Moench to saline-alkali stress. PLoS One. 2019;14(7):e0220340. [CrossRef].
6. Guo R, Yang Z, Li F, Yan C, Zhong X, Liu Q, et al. Comparative metabolic responses and adaptive strategies of wheat (*Triticum aestivum*) to salt and alkali stress. BMC Plant Biol. 2015;15:170. [CrossRef].
7. Liu X, Wang B, Zhao Y, Chu M, Yu H, Gao D, et al. Physiological and transcriptional responses of sorghum seedlings under alkali stress. Plants. 2025;14(19):3106. [CrossRef].
8. Muchate NS, Nikalje GC, Rajurkar NS, Suprasanna P, Nikam TD. Plant salt stress: adaptive responses, tolerance mechanism and bioengineering for salt tolerance. Bot Rev. 2016;82(4):371–406. [CrossRef].
9. Li Z, Zhu L, Zhao F, Li J, Zhang X, Kong X, et al. Plant salinity stress response and nano-enabled plant salt tolerance. Front Plant Sci. 2022;13:843994. [CrossRef].
10. Etesami H, Fatemi H, Rizwan M. Interactions of nanoparticles and salinity stress at physiological, biochemical and molecular levels in plants: a review. Ecotoxicol Environ Saf. 2021;225:112769. [CrossRef].
11. Kopittke PM, Lombi E, Wang P, Schjoerring JK, Husted S. Nanomaterials as fertilizers for improving plant mineral nutrition and environmental outcomes. Environ Sci Nano. 2019;6(12):3513–24. [CrossRef].
12. Nair R, Varghese SH, Nair BG, Maekawa T, Yoshida Y, Kumar DS. Nanoparticulate material delivery to plants. Plant Sci. 2010;179(3):154–63. [CrossRef].
13. Lv J, Christie P, Zhang S. Uptake, translocation, and transformation of metal-based nanoparticles in plants: recent advances and methodological challenges. Environ Sci Nano. 2019;6(1):41–59. [CrossRef].
14. Alharbi K, Hafez EM, Omara AE, Rashwan E, Alshaal T. Zinc oxide nanoparticles and PGPR strengthen salinity tolerance and productivity of wheat irrigated with saline water in sodic-saline soil. Plant Soil. 2023;493(1):475–95. [CrossRef].
15. Faizan M, Bhat JA, Chen C, Alyemeni MN, Wijaya L, Ahmad P, et al. Zinc oxide nanoparticles (ZnO-NPs) induce salt tolerance by improving the antioxidant system and photosynthetic machinery in tomato. Plant Physiol Biochem. 2021;161:122–30. [CrossRef].

16. Singh A, Rajput VD, Lalotra S, Agrawal S, Ghazaryan K, Singh J, et al. Zinc oxide nanoparticles influence on plant tolerance to salinity stress: insights into physiological, biochemical, and molecular responses. Environ Geochem Health. 2024;46(5):148. [CrossRef].
17. Singh A, Rajput VD, Sharma R, Ghazaryan K, Minkina T. Salinity stress and nanoparticles: insights into antioxidative enzymatic resistance, signaling, and defense mechanisms. Environ Res. 2023;235:116585. [CrossRef].
18. Verma N, Kaushal P, Gahalot D, Sidhu AK, Kaur K. Mechanistic aspect of zinc oxide nanoparticles in alleviating abiotic stress in plants—a sustainable agriculture approach. BioNanoScience. 2023;13(4):1645–61. [CrossRef].
19. Adil M, Bashir S, Bashir S, Aslam Z, Ahmad N, Younas T, et al. Zinc oxide nanoparticles improved chlorophyll contents, physical parameters, and wheat yield under salt stress. Front Plant Sci. 2022;13:932861. [CrossRef].
20. Elshoky HA, Yotsova E, Farghali MA, Farroh KY, El-Sayed K, Elzorkany HE, et al. Impact of foliar spray of zinc oxide nanoparticles on the photosynthesis of *Pisum* sativum L. under salt stress. Plant Physiol Biochem. 2021;167:607–18. [CrossRef].
21. Gaafar RM, Diab RH, Halawa MI, Elshanshory A, El-Shaer A, Hamouda MM. Role of zinc oxide nanoparticles in ameliorating salt tolerance in soybean. Egypt J Bot. 2020;60(3):733–47. [CrossRef].
22. Mustafa G, Chaudhari SK, Manzoor M, Batool S, Hatami M, Hasan M. Zinc oxide nanoparticles mediated salinity stress mitigation in *Pisum* sativum: a physio-biochemical perspective. BMC Plant Biol. 2024;24(1):835. [CrossRef].
23. Singh A, Sengar RS, Rajput VD, Minkina T, Singh RK. Zinc oxide nanoparticles improve salt tolerance in rice seedlings by improving physiological and biochemical indices. Agriculture. 2022;12(7):1014. [CrossRef].
24. Aregawi K, Shen J, Pierroz G, Sharma MK, Dahlberg J, Owiti J, et al. Morphogene-assisted transformation of Sorghum bicolor allows more efficient genome editing. Plant Biotechnol J. 2022;20(4):748–60. [CrossRef].
25. Ochieng G, Ngugi K, Wamalwa LN, Manyasa E, Muchira N, Nyamongo D, et al. Novel sources of drought tolerance from landraces and wild sorghum relatives. Crop Sci. 2021;61(1):104–18. [CrossRef].
26. Dourado PRM, de Souza ER, dos Santos MA, Lins CMT, Monteiro DR, Paulino MKSS, et al. Stomatal regulation and osmotic adjustment in sorghum in response to salinity. Agriculture. 2022;12(5):658. [CrossRef].
27. Dehnavi AR, Zahedi M, Ludwiczak A, Perez SC, Piernik A. Effect of salinity on seed germination and seedling development of sorghum (*Sorghum bicolor* (L.) Moench) genotypes. Agronomy. 2020;10(6):859. [CrossRef].
28. Maswada HF, Djanaguiraman M, Prasad PVV. Seed treatment with nano-iron (III) oxide enhances germination, seeding growth and salinity tolerance of sorghum. J Agron Crop Sci. 2018;204(6):577–87. [CrossRef].
29. Chen X, Zhang R, Xing Y, Jiang B, Li B, Xu X, et al. The efficacy of different seed priming agents for promoting sorghum germination under salt stress. PLoS One. 2021;16(1):e0245505. [CrossRef].
30. Diao J, Tang Y, Jiang Y, Sun H, Zhang CJ. Using nanomaterials and arbuscular mycorrhizas to alleviate saline–alkali stress in *Cyperus esculentus* (L.). Agronomy. 2024;14(11):2476. [CrossRef].
31. Xian X, Zhang Z, Li C, Ding L, Guo H, Zhai J, et al. Comprehensive analysis revealed that titanium dioxide nanoparticles could strengthen the resistance of apple rootstock B9 to saline-alkali stress. Funct Plant Biol. 2023;51:FP23126. [CrossRef].
32. Wang C, Wei X, Wang Y, Wu C, Jiao P, Jiang Z, et al. Metabolomics and transcriptomic analysis revealed the response mechanism of maize to saline-alkali stress. Plant Biotechnol J. 2025;23(12):5397–416. [CrossRef].
33. Wu R, Kong L, Wu X, Gao J, Niu T, Li J, et al. GsNAC2 gene enhances saline-alkali stress tolerance by promoting plant growth and regulating glutathione metabolism in Sorghum bicolor. Funct Plant Biol. 2023;50(9):677–90. [CrossRef].
34. Hiscox JD, Israelstam GF. A method for the extraction of chlorophyll from leaf tissue without maceration. Can J Bot. 1979;57(12):1332–4. [CrossRef].
35. Wellburn AR. The spectral determination of chlorophylls a and b, as well as total carotenoids, using various solvents with spectrophotometers of different resolution. J Plant Physiol. 1994;144(3):307–13. [CrossRef].
36. Ramzan M, Naz G, Ali shah A, Parveen M, Jamil M, Gill S, et al. Synthesis of phytostabilized zinc oxide nanoparticles and their effects on physiological and anti-oxidative responses of *Zea mays* (L.) under chromium stress. Plant Physiol Biochem. 2023;196:130–8. [CrossRef].
37. Zhang WF, Zhang F, Raziuddin R, Gong HJ, Yang ZM, Lu L, et al. Effects of 5-aminolevulinic acid on oilseed rape seedling growth under herbicide toxicity stress. J Plant Growth Regul. 2008;27(2):159–69. [CrossRef].

38. Samadi S, Saharkhiz MJ, Azizi M, Samiei L, Karami A, Ghorbanpour M. Single-wall carbon nano tubes (SWCNTs) penetrate Thymus daenensis Celak. plant cells and increase secondary metabolite accumulation *in vitro*. Ind Crops Prod. 2021;165:113424. [CrossRef].
39. Glick D, Maehly A. Assay of catalases and peroxidases. Methods Biochem Anal. 1955;10:9780470110171. [CrossRef].
40. Khaleghi A, Naderi R, Brunetti C, Maserti BE, Salami SA, Babalar M. Morphological, physiochemical and antioxidant responses of *Maclura pomifera* to drought stress. Sci Rep. 2019;9(1):19250. [CrossRef].
41. Huang C, He W, Guo J, Chang X, Su P, Zhang L. Increased sensitivity to salt stress in an ascorbate-deficient *Arabidopsis mutant*. J Exp Bot. 2005;56(422):3041–9. [CrossRef].
42. Feng N, Yu M, Li Y, Jin D, Zheng D. Prohexadione-calcium alleviates saline-alkali stress in soybean seedlings by improving the photosynthesis and up-regulating antioxidant defense. Ecotoxicol Environ Saf. 2021;220:112369. [CrossRef].
43. Tanveer Y, Jahangir S, Shah ZA, Yasmin H, Nosheen A, Hassan MN, et al. Zinc oxide nanoparticles mediated biostimulant impact on cadmium detoxification and *in silico* analysis of zinc oxide-cadmium networks in *Zea mays* L. regulome. Environ Pollut. 2023;316(Pt 2):120641. [CrossRef].
44. Barin JS, Pereira JSF, Mello PA, Knorr CL, Moraes DP, Mesko MF, et al. Focused microwave-induced combustion for digestion of botanical samples and metals determination by ICP OES and ICP-MS. Talanta. 2012;94:308–14. [CrossRef].
45. Yang Q, Yu H, Yang C, Zhao Z, Ju Z, Wang J, et al. Enhanced phytoremediation of cadmium-contaminated soil using chelating agents and plant growth regulators: effect and mechanism. R Soc Open Sci. 2024;11(9):240672. [CrossRef].
46. Chen Z, Wang Q. Graphene ameliorates saline-alkaline stress-induced damage and improves growth and tolerance in alfalfa (*Medicago sativa* L.). Plant Physiol Biochem. 2021;163:128–38. [CrossRef].
47. Iftikhar M, Ali Shah A. Green-synthesized ZnO and MgO nanoparticles modulate physiology and antioxidant defense in maize under alkaline stress. Funct Plant Biol. 2025;52(10):FP25200. [CrossRef].
48. Rakgotho T, Ndou N, Mulaudzi T, Iwuoha E, Mayedwa N, Ajayi RF. Green-synthesized zinc oxide nanoparticles mitigate salt stress in sorghum bicolor. Agriculture. 2022;12(5):597. [CrossRef].
49. Zhang H, Zhao Y, Zhu JK. Thriving under stress: how plants balance growth and the stress response. Dev Cell. 2020;55(5):529–43. [CrossRef].
50. Seleiman MF, Ahmad A, Alhammad BA, Tola E. Exogenous application of zinc oxide nanoparticles improved antioxidants, photosynthetic, and yield traits in salt-stressed maize. Agronomy. 2023;13(10):2645. [CrossRef].
51. Zhai J, Xian X, Zhang Z, Wang Y. Nano-zinc oxide can enhance the tolerance of apple rootstock M9-T337 seedlings to saline alkali stress by initiating a variety of physiological and biochemical pathways. Plants. 2025;14(2):233. [CrossRef].
52. Zhou H, Shi H, Yang Y, Feng X, Chen X, Xiao F, et al. Insights into plant salt stress signaling and tolerance. J Genet Genomics. 2024;51(1):16–34. [CrossRef].
53. Dumanović J, Nepovimova E, Natić M, Kuča K, Jaćević V. The significance of reactive oxygen species and antioxidant defense system in plants: a concise overview. Front Plant Sci. 2021;11:552969. [CrossRef].
54. Qian J, Shan R, Shi Y, Li H, Xue L, Song Y, et al. Zinc oxide nanoparticles alleviate salt stress in cotton (*Gossypium hirsutum* L.) by adjusting Na^+/K^+ ratio and antioxidative ability. Life. 2024;14(5):595. [CrossRef].
55. Chen K, Hao M, Yuan T, Chai S, Su G, Wu C, et al. Biosynthesized Fe-C-dots nanozymes modulate growth, physiological and phytochemical peculiarity to improve saline-alkaline stress tolerance in wheat. Plant Physiol Biochem. 2025;222:109777. [CrossRef].
56. Singh A, Sengar RS, Shahi UP, Rajput VD, Minkina T, Ghazaryan KA. Prominent effects of zinc oxide nanoparticles on roots of rice (*Oryza sativa* L.) grown under salinity stress. Stresses. 2022;3(1):33–46. [CrossRef].
57. Türkoğlu A, Haliloğlu K, Ekinci M, Turan M, Yildirim E, Öztürk Hİ, et al. Zinc oxide nanoparticles: an influential element in alleviating salt stress in quinoa (*Chenopodium quinoa* L. cv atlas). Agronomy. 2024;14(7):1462. [CrossRef].
58. Olatunbosun A, Nigar H, Rovshan K, Nurlan A, Boyukhanim J, Narmina A, et al. Comparative impact of nanoparticles on salt resistance of wheat plants. MethodsX. 2023;11:102371. [CrossRef].

59. Rajput V, Minkina T, Ahmed B, Sushkova S, Singh R, Soldatov M, et al. Interaction of copper-based nanoparticles to soil, terrestrial, and aquatic systems: critical review of the state of the science and future perspectives. In: de Voogt P, editor. Reviews of environmental contamination and toxicology, Vol. 252. Berlin/Heidelberg, Germany: Springer; 2020. p. 51–96. [CrossRef].
60. Strekalovskaya EI, Perfileva AI, Krutovsky KV. Zinc oxide nanoparticles in the “soil–bacterial community–plant” system: impact on the stability of soil ecosystems. Agronomy. 2024;14(7):1588. [CrossRef].
61. Shah GM, Shabbir Z, Rabbani F, Rashid MI, Bakhat HF, Naeem MA, et al. Soil texture mediates the toxicity of ZnO and Fe_3O_4 nanoparticles to microbial activity. Toxics. 2025;13(2):84. [CrossRef].
62. Markowicz A, Borymski S, Adamek A, Sułowicz S. The influence of ZnO nanoparticles on horizontal transfer of resistance genes in lab and soil conditions. Environ Res. 2023;223:115420. [CrossRef].